Mathematical Biosciences and Engineering

Research article

Segmentation and identification of spectral and statistical textures for computer medical diagnostics in dermatology

Xinlin Liu[1], Viktor Krylov[2], Su Jun[1], Natalya Volkova[2], Anatoliy Sachenko[3,4,*], Galina Shcherbakova[5] and Jacek Woloszyn[3]

[1] School of Computer Science, Hubei University of Technology, Wuhan 430068, China
[2] Department of Applied Mathematics and Information Technologies, Odessa National Polytechnic University, Odessa 65044, Ukraine
[3] Department of Informatics and Teleinformatics, Kazimierz Pulaski University of Technology and Humanities in Radom, Radom 26600, Poland
[4] Research Institute for Intelligent Computer Systems, West Ukrainian National University, Ternopil 46009, Ukraine
[5] Department of Information Systems, Odessa National Polytechnic University, Odessa 65044, Ukraine

* Correspondence: Email: as@wunu.edu.ua; Tel: +380974313425; Fax: +380352475053.

Abstract: An important component of the computer systems of medical diagnostics in dermatology is the device for recognition of visual images (DRVI), which includes identification and segmentation procedures to build the image of the object for recognition. In this study, the peculiarities of the application of detection, classification and vector-difference approaches for the segmentation of textures of different types in images of dermatological diseases were considered. To increase the quality of segmented images in dermatologic diagnostic systems using a DRVI, an improved vector-difference method for spectral-statistical texture segmentation has been developed. The method is based on the estimation of the number of features and subsequent calculation of a specific texture feature, and it uses wavelets obtained by transforming the graph of the power function at the stage of contour segmentation. Based on the above, the authors developed a modulus for spectral-statistical texture segmentation, which they applied to segment images of psoriatic disease; the Pratt's criterion was used to assess the quality of segmentation. The reliability of the classification of the spectral-statistical texture images was confirmed by using the True Positive Rate (TPR) and False Positive Rate (FPR) metrics calculated on the basis of the confusion matrix. The results of the experimental research confirmed the advantage of the proposed vector-difference

method for the segmentation of spectral-statistical textures. The method enables further supplementation of the vector of features at the stage of identification through the use of the most informative features based on characteristic points for different degrees and types of psoriatic disease.

Keywords: identification; textural segmentation; spectral-statistical texture; vector-difference approach; wavelets; characteristic points

1. Introduction

In one of the oldest branches of medical science, i.e., dermatology exists a number of diseases in which early diagnosis is very important, and a significant part of humanity suffers from such diseases. For example, psoriasis affects about 3–4% of the population of our planet [1], and new cases of melanoma in the United States of America are registered to be more than 80 thousand per year [2]. A diagnosis at the early stage can either increase the likelihood of being cured (for melanoma) or reduce the likelihood of serious complications (for psoriasis). The severity of the disease allows us to assess quantitative measurements. For example, Psoriasis Area and Severity index (PASI) is often used by specialists in the clinical practice [3,4]. However, its calculation is a time-consuming process, with a high probability of subjective estimates. Therefore, the medical diagnostic systems in dermatology take an important role, increasing the efficiency and reliability of diagnosis.

The intelligent DRVI [5–7] is an important part of these systems above. The basic processes of medical diagnostic systems in dermatology are segmentation and identification. The purpose of segmentation is to reduce the amount of data processed for identification to determine the vector of features. These procedures should provide the quality of classification, the reliability of diagnostic solutions and the efficiency of image processing in DRVIs [8–10].

In segmentation, the data are combined to form segments according to one or more features, such as color, intensity and texture [11]. Texture segmentation is quite difficult in the diagnosis of such diseases as psoriasis, eczema and atopic dermatitis [4,8,9]. The quality of texture segmentation affects the reliability of diagnostic solutions in general.

For the implementation of the texture segmentation procedure in DRVI detection, classification methods are most used [12,13]. Detection methods include the following processes: the assessment of the sign of segmentation, the emphasis of the border between homogeneous areas in the image and the threshold and morphological processing of potential boundaries for homogeneous textural areas. Using detection methods, the segmentation is performed on the basis of one feature. This feature is converted into intensity and taken into account when determining the boundaries of homogeneous texture areas by using methods of contour segmentation. The advantage of detection methods is the simplicity of implementation and high efficiency of image processing. However, these methods are characterized by low noise immunity.

When using classification methods, the segmentation feature(s) is (are) assessed, the feature vectors are classified, the boundary points of homogeneous areas are selected and the boundaries are processed. Segmentation via classification methods is carried out according to several criteria. These methods allow segmentation to be applied to a wider class of images and textures [11]. The quality of the segmentation is determined by coincidence of borders for actually selected segmented

homogeneous texture area and the pre-marked one. An advantage of classification methods is the high quality of segmentation. The disadvantages are the low efficiency of image processing and the need for a large training sample to ensure reliable classification.

The selection of the particular segmentation method depends on the type of texture model. The known types of textures are statistical and spectral. A distinctive feature of spectral texture models is that they can be described as a quasi-periodic signal. Statistical texture models assess the presence or absence of the spatial interaction between non-derivative textural elements. However, when diagnosing the characteristics of a number of dermatological diseases, such as the degree of psoriasis, a combined spectral-statistical type of texture can be used [14–16]. In this case, the psoriatic plaque looks like a red spot that is covered with large silvery-white scales and paraffin flakes. For these types of textures, employing detection and classification methods in texture segmentation does not provide the quality of segmentation necessary for practical use.

Selecting the type of texture model usually determines the approach for finding the features of the texture for subsequent identification. Statistical texture models make it possible to determine the moments and features of images for different ranges; for example, R, G, B, and/or features obtained on their basis (entropy, contrast, homogeneity, etc.) [17] often use the matrices of coincidences or energy characteristics [18]. Spectral texture models represent texture in terms of spatial frequency and allow spectral descriptors to be determined using Fourier spectra, the amplitude spectrum of which differs for textures according to the frequency characteristics and some statistical descriptors [19]; for example, the autocorrelation function can supplement the vector of features. The disadvantages of these approaches are that they require an additional investigation to select the calculation parameters and a sufficient set of features invariant to shifting and rotation, which is a characteristic feature for the application of noise levels.

Today, to determine the severity of psoriasis, doctors usually use one of the many known indices (PASI, BSA (Body Surface Area), etc.) [6,8]. The most popular among them is the PASI [3,6]. A significant number of these indices need the diseased areas to be determined. The calculation of the PASI takes into account the numerical ratio and area of the relevant parts of the human body, as well as the assessment of psoriasis signs, which are determined by a dermatologist and include erythema, peeling and infiltration. However, the PASI is characterized by a lack of nonlinearity. This disadvantage is especially significant with low PASI values, i.e., when determining whether a patient has the disease at all. A reliable answer to this question is especially important when diagnosing. This should be facilitated using the approach to determine the geometric moments and features [20], which are invariant to the parallel transfer and rotation angle of the object (i.e., scaling-resistant).

The analysis of the domain above shows that the existing medical diagnostic systems in dermatology do not provide the necessary reliability and/or efficiency. In addition, the efficiency of processing and the reliability of diagnostic solutions are largely determined by the quality of the segmentation of the medical and biological images to be processed. A significant number of such images are of combined spectral-statistical nature.

Among the most significant shortcomings of existing segmentation methods, we consider the following ones: the low quality of detection methods and the need for a large training sample to ensure the quality of classification methods for hybrid types of textures. Existing identification methods introduce errors into the calculation of the known indices when determining the degree of psoriasis.

Therefore, the authors aimed to increase the quality of segmentation by 1) improving the

models of spectral-statistical textures, 2) developing an improved method for the segmentation of spectral-statistical textures and 3) designing the procedure for determining the vector of features to ensure sufficient quality classification, the reliability of the diagnostic solutions and the efficiency of image processing in DRVIs. In particular, it is expected to take into account the values of statistical and spectral textural features and determine the geometric moments and features on the basis of the results of calculating the characteristic points of the contours during the formation of the vector of features; at the stage of contour segmentation, apply the method using wavelets obtained by transforming the power graph.

2. Materials and methods

As mentioned above, the texture of dermatological disease images can be of spectral, statistical or combined spectral-statistical nature [14–16]. For such types of textures, an improved vector-difference method of texture segmentation has been developed. It is based on idea of determining the modulus of the difference of vectors, the elements of which are the values of textural features, to convert the image of the texture into intensity. To assess the quality of segmentation, the Pratt's criterion [21,22] is used to compare the boundaries of perfectly and actually segmented textured images:

$$R = (1/I) \sum_{i=1}^{I_A} 1/(1 + \alpha d_i^2), \qquad (1)$$

where $I = \max(I_i, I_p)$; I_i, I_p—the number of points on the boundary of the segments of perfectly and actually segmented images, respectively; α—scaling constant, usually set to $1/9$; d_i—the distance between the boundary point of the actually segmented image and the line that includes the points of ideal boundary of the segment.

The improved vector-difference method for texture segmentation includes the stages of image scanning using the processing window, identification, vector-difference transformation and contour segmentation. At the stage of identification, the primary identification vector is built.

The calculation of the values for the textural features is performed in the sliding window whose size is chosen according to the purpose of the processing task. This paper proposes the development of the method given in [21]. When performing the identification, the identification vector of features j for each i-th pixel of the image in the processing aperture $\vec{c}_i(c_{1,i}, c_{2,i}, \dots, c_{n,i})$ is received, where $j = \overline{1, n}$ and n is a number of features.

The construction of the identification vector involves two stages:

1) Calculating the difference of vectors in the $(i + 1)$-th and i-th pixels of the image, i.e., determining the difference between $\overrightarrow{c}_{i+1}(c_{1,i+1}, c_{2,i+1}, \dots, c_{n,i+1})$ and $\overrightarrow{c}_i(c_{1,i}, c_{2,i}, \dots, c_{n,i})$.

2) Calculating the modulus of the difference between two vectors $\overrightarrow{c}_{i+1}(c_{1,i+1}, c_{2,i+1}, \dots, c_{n,i+1})$ and $\overrightarrow{c}_i(c_{1,i}, c_{2,i}, \dots, c_{n,i})$ using methods of vector algebra, as follows:

$$\vec{c} = \left| \overrightarrow{c}_{i+1}(c_{1,i+1}, c_{2,i+1}, \dots, c_{n,i+1}) - \overrightarrow{c}_i(c_{1,i}, c_{2,i}, \dots, c_{n,i}) \right| = \qquad (2)$$

$$= \overrightarrow{(c_{1,i+1} - c_{1,i}, c_{2,i+1} - c_{2,i}, \dots, c_{n,i+1} - c_{n,i})}.$$

Then, the techniques of the contour segmentation are used [15,16].

Since the proposed method has features of both detection and classification approaches and the latter requires a representative training sample for its formation, a previously developed spectral-

statistical texture model [21] was improved; it is described by the expression (5) below.

When modeling the spectral texture, the spatial-frequency properties of the variation of the intensity of the image pixels are taken into account [23]. Spectral texture models are characterized by the value of the background component and the change in spatial frequency. Then, the value of the intensity of the m-th row of the spectral textured image is represented as a combination of segments that do not intersect, as follows:

$$I(x, y_m) = \cup_{i=1}^{k}\{c_i(x, y_m) + \sum_{j=1}^{n} A_{ij}(x, y_m)\sin(\omega_m^{ij}x)\}, \; x \in [q_{i-1}, q_i], \qquad (3)$$

where $A_{ij}(x, y_m), \omega_m^{ij}$—the amplitude and frequency of the j-th modulated oscillation on the i-th segment of the m-th image; $c_i(x, y_m)$—a representation of the background on the i-th segment for the m-th row of the image; $q = (q_0, ..., q_{k+1})$—a vector of boundaries of textured areas for the m-th row of the image when $q_0 = 1$ and $q_{k+1} = N + 1$, where N is the number of pixels in the image row; $x = 1, ..., N; y = 1, ..., M$, where M represents the spatial coordinates.

The statistical texture models take into account the values of the background component and indicators of variation for the random field. The intensity of the m-th row for the image of the statistical texture is represented as a combination of segments that do not intersect, as follows:

$$I(x, y_m) = \cup_{i=1}^{k}\{c_i(x, y_m) + N_i(x, y_m)\}, \; x \in [q_{i-1}, q_i], \qquad (4)$$

where $N_i(x, y_m)$—Gaussian noise with zero mean and variance σ_i^2 on the i-th segment of the image.

The combined spectral-statistical texture model is characterized by the background component value, the random change in spatial frequency and random field variations. The intensity of the m-th row for the spectral-statistical model of texture is represented as follows:

$$I(x, y_m) = \cup_{i=1}^{k}\{c_i(x, y_m) + N_i(x, y_m) + \sum_{j=1}^{n} A_{ij}(x, y_m)\sin(\omega_m^{ij}x)\}, \; x \in [q_{i-1}, q_i], \qquad (5)$$

where $N_i(x, y_m)$—Gaussian noise with zero mean and variance σ_i^2 on the i-th segment of the image.

Taking into account the above given mathematical model of textures, to construct the image of the spectral-statistical texture, the method for identification of the spectral-statistical texture is proposed, whereby an identification vector is constructed; it is a combination of spectral and statistical textural features.

It is proposed to define each element of the vector for the statistical textural features as follows:

1) The processing aperture is formed for each pixel of an image of size M. The size of the processing aperture is selected depending on the purpose of the processing task.

2) In each row of the image matrix in the processing aperture for each pixel, the calculation of the average pixel intensity is performed as follows:

$$\bar{I} = \frac{\sum_{i=1}^{M} I_i}{M}. \qquad (6)$$

3) The statistical variance estimate is defined for each processing aperture per each pixel by applying the following quadratic-amplitude transformation:

$$\overline{\sigma} = \frac{\sum_{i=1}^{M}(I_i - \overline{I})^2}{M}, \tag{7}$$

where $I_i > \overline{I}, i = \overline{1, M}$.

The following algorithm can define each element of the feature vector for the spectral texture:

1) A processing aperture of size M is formed for each pixel of the image. The size of the processing aperture is chosen depending on the purpose of the processing task.

2) A direct Fourier transform is performed in each row of the image matrix in the processing aperture of each image pixel, as follows:

$$\hat{I}(\omega) = \frac{1}{M}\sum_{x_i=1}^{M-1} I(x_i, y_m) e^{-j2\pi\omega x_i/M}, \tag{8}$$

where $\omega = \overline{0, M-1}$.

3) A linear frequency conversion is carried out for each processing aperture of each pixel: $z(\omega) = k \cdot \hat{I}(\omega)$, and, as a result, the spectral composition of the texture changes to scattered.

4) The inverse Fourier transform is performed $I(x_i, y_m) = \sum_{\omega=1}^{M-1} z(\omega) e^{j2\pi\omega x_i/M}$, $x_i = \overline{0, M-1}$.

5) The statistical estimate of the numerical characteristics of the scatter for each image pixel in the processing aperture is calculated according to (7).

The results of calculating the spectral texture of the psoriasis image are shown in Figure 1.

a)   b)
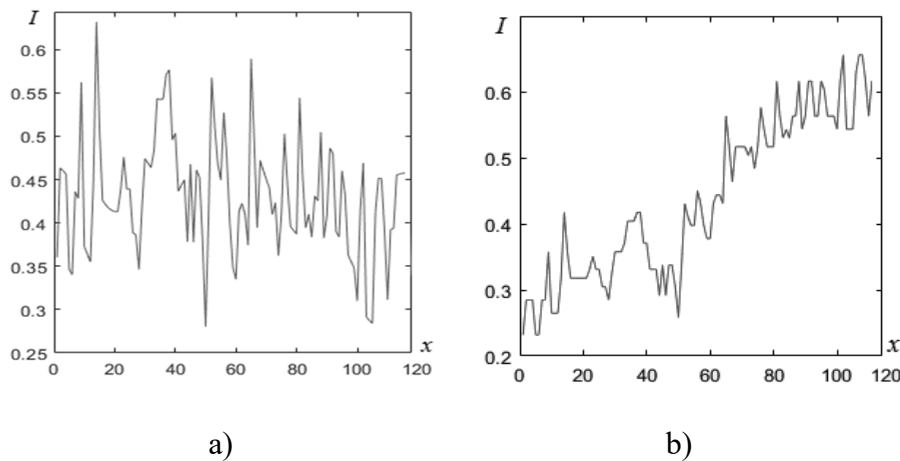
Figure 1. Results of calculating the value of the spectral textural feature: the row of the input psoriasis image a) after the quadratic-amplitude transformation b).

According to (2), the spectral-statistical textural feature $\overrightarrow{\sigma_r}$ was calculated as the modulus of the difference of two vectors, with the preliminary normalization of the values of the statistical $\overrightarrow{\sigma_i}$ and spectral $\overrightarrow{\sigma_{i+1}}$ textures being performed according to their maximum values:

$$\overrightarrow{\sigma_i} = \frac{\overrightarrow{\sigma_i}}{\overrightarrow{\sigma_{i,\max}}}, \overrightarrow{\sigma_{i+1}} = \frac{\overrightarrow{\sigma_{i+1}}}{\overrightarrow{\sigma_{i+1,\max}}}, \tag{9}$$

where $\overrightarrow{\sigma_{i,\max}}$ and $\overrightarrow{\sigma_{i+1,\max}}$—the maximum values of the variation features of the statistical and spectral textures, respectively.

During the study, a sample of 30 model images of spectral-statistical textures was constructed according to (5). The size of the images was 512×512, and the pixel intensity of the images varied from 0 to 255. Each model image contained two areas with different frequencies ω_1 and ω_2 (period/degree), and the amplitude $A = 1$; the random change of amplitude and frequency occurred due to the superimposition of the Gaussian noise with a zero mean and the varying Gaussian interference for different image segments. The reliability of the classification method for homogeneous areas of test images with different levels of interference under the conditions of identifying spectral and statistical textures (concurrently and separately) based on the confusion matrix was estimated (Table 1). It was performed using the *TPR* metrics, which measure the probability for the correct detection of texture pixels, and the *FPR* metrics that measure the reliability of the erroneous assignment of pixels to the spectral-statistical texture area if they do not really belong to this area (i.e., the probability of the false alarm) (Table 2).

The results of comparative analysis are shown in Table 2 for the identification on the basis of the spectral and statistical texture; the authors confirmed the following outcomes. The probability for the correct detection of the spectral-statistical texture (*TPR*) was not less than 1.6 times more than one based on the spectral texture, and it was not less than six times more than one based on the statistical texture at a signal-to-noise ratio equal to 5 or more. The probability of the false alarm (*FPR*) was less than 0.4 when the signal-to-noise ratio was less than 5, and it was not more than 0.06 when the signal-to-noise ratio was more than 5.

Table 1. Confusion matrix when identifying the model image (5) using different signal-to-noise ratios given as *q*.

Test image markup	*q*	Image markup on the basis of spectral and statistical textures, %		Image markup on the basis of spectral texture, %		Image markup on the basis of statistical texture, %	
		Area 1	Area 2	Area 1	Area 2	Area 1	Area 2
Area 1	1	54.14	45.86	89.42	10.58	69.37	30.63
Area 2		36.54	63.46	72.29	27.70	34.05	65.95
Area 1	2	52.76	47.24	96.21	3.79	72.36	27.64
Area 2		36.91	63.09	77.12	22.88	35.09	64.90
Area 1	5	71.89	28.10	93.77	6.23	67.29	32.71
Area 2		39.62	60.39	60.78	39.22	34.87	65.13
Area 1	10	95.39	4.60	80.74	19.26	80.74	42.92
Area 2		35.74	64.26	38.14	61.86	39.82	60.18
Area 1	20	95.05	4.95	81.44	18.56	40.18	59.82
Area 2		19.48	80.52	28.27	71.73	47.07	52.93
Area 1	50	93.82	6.18	83.69	16.30	18.07	81.93
Area 2		12.38	87.61	15.42	84.58	51.09	48.91
Area 1	100	94.54	5.46	87.35	12.65	15.31	84.69
Area 2		1.95	98.05	11.46	88.54	53.36	46.64

Table 2. Results of determining the reliability of the classification for homogeneous areas by applying the TPR metric using different signal-to-noise ratios.

Signal-to-noise ratio	On the basis of spectral and statistical textures	On the basis of spectral texture	On the basis of statistical texture
1	0.59	0.56	0.68
2	0.58	0.55	0.67
5	0.64	0.60	0.65
10	0.73	0.67	0.66
20	0.83	0.74	0.46
50	0.88	0.84	0.26
100	0.97	0.88	0.22

Based on [21] and the proposed method for the identification of spectral-statistical textures, the improved vector-difference method of spectral-statistical texture was developed. To implement this method, contour segmentation was applied using wavelets obtained by transforming the graph of the power function, as they are characterized by a low error associated with determining the coordinates of intensity difference points for the underlying transformation [24].

The improved segmentation method for spectral-statistical textures includes the following stages:

1) Calculating the feature values of the statistical texture c_1 (numerical characteristics of statistical texture scatter) and spectral textural features c_2 (numerical characteristic of spectral texture scatter) for the i-th pixel of the image in the processing aperture.

2) Generating the identification vector of features for each i-th pixel of the image in processing aperture $\overrightarrow{c}_i(c_{1,i}, c_{2,i})$ in the feature space.

3) Calculating the difference between the vectors in the $(i + 1)$-th and i-th pixels of the image, i.e., calculating the difference between the following vectors (2): $\overrightarrow{c}_{i+1}(c_{1,i+1}, c_{2,i+1})$ and $\overrightarrow{c}_i(c_{1,i}, c_{2,i})$.

4) Calculating the modulus of the difference between two vectors $\overrightarrow{c}_{i+1}(c_{1,i+1}, c_{2,i+1})$ and $\overrightarrow{c}_i(c_{1,i}, c_{2,i})$.

5) Contour segmentation using wavelets obtained by transforming the graph of the power function [24].
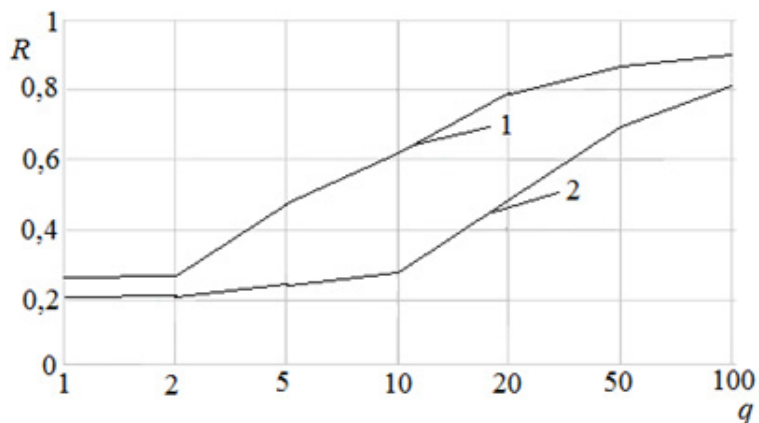
3.   Experiment and results

An experimental study of the improved vector-difference segmentation method was carried out; the stage of contour segmentation wavelets obtained by transforming the graph of the power function [21] were used. For the segmentation of the test images of the spectral-statistical texture (Figure 2) at different signal-to-noise ratios, the improved method was applied at the stage of the contour segmentation using wavelets obtained by transforming the graph of power function ($s < 1$) and employing the Canny method. Figure 2 shows the results of applying the improved method and the original method [21] to the test image at a signal-to-noise ratio of 20.

a)   b)   c)
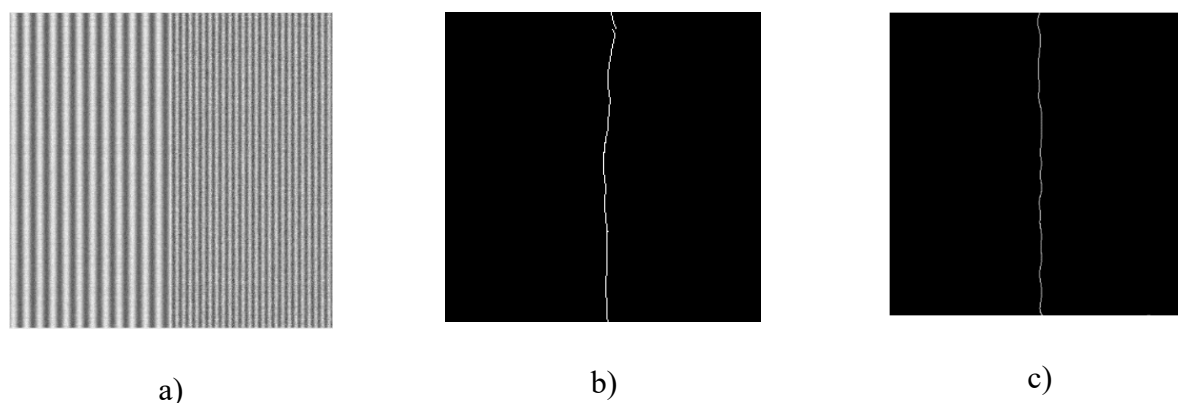
Figure 2. Results of test image segmentation: a) test image at the ratio of signal-to-noise $q = 20$; b) image obtained using the method in [21]; c) image obtained using the improved method.

To determine the quality of segmentation with different values of the signal-to-noise ratio, the Pratt's criterion (1) was used and the graphs for the dependence of the Pratt's criterion indicator on the signal-to-noise ratio for the improved method and original method [21] were constructed (Figure 3). It was found that, at the signal-to-noise ratio $q > 5$, the improved method for texture segmentation using wavelets obtained by transforming the graph of the power function outperformed the segmentation quality of the original method [21] by 1.1–1.2 times.

Figure 3. Dependence of the Pratt's criterion on the signal-to-noise ratio: 1—results for the improved vector-difference method using wavelets obtained by transforming the graph of the power function at the stage of contour segmentation; 2—results for the original method [21].

The segmentation modulus of the spectral-statistical textures based on the improved vector-difference segmentation method for DRVIs in medical diagnostic systems was developed (Figure 4).
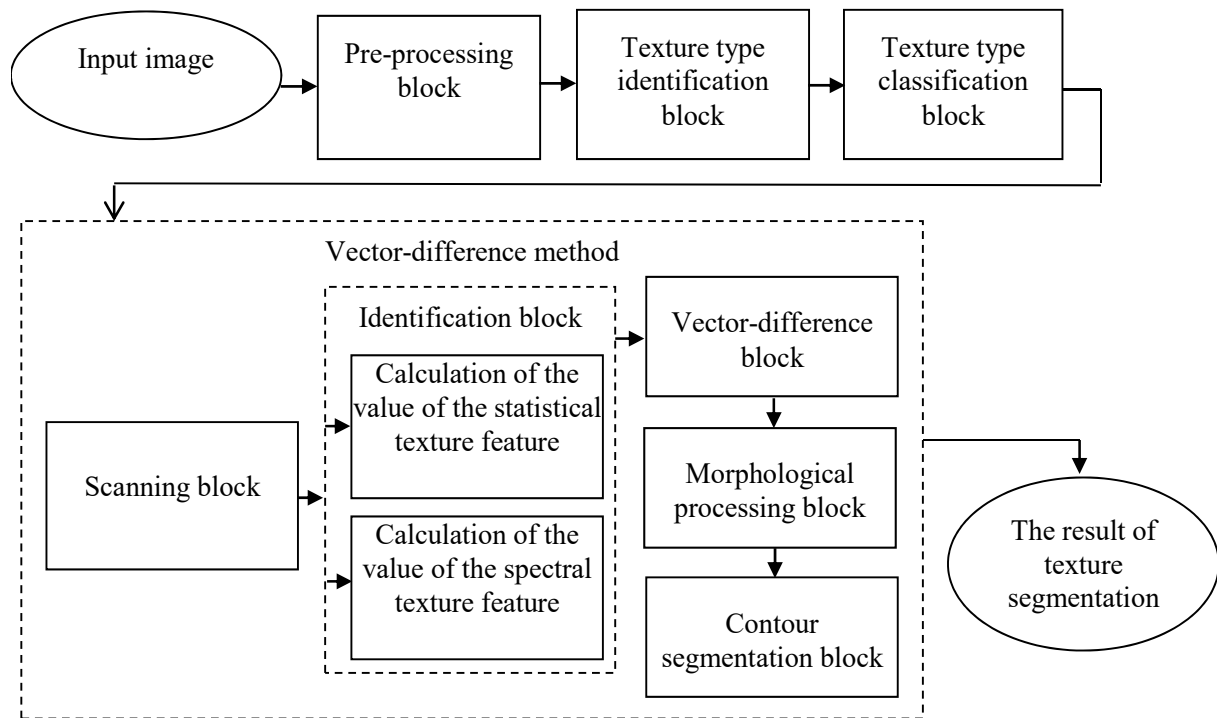
Figure 4. Modulus of spectral-statistical texture segmentation for DRVIs.

According to the block diagram (Figure 4), the input image of the recognition object (Figure 5) enters the pre-processing block. In this block, a homomorphic filter is used to remove the multiplicative noise that occurs due to the uneven illumination of the object when the image is received. The processed image enters the texture-type identification block, where the type of texture is identified using the method of texture identification based on multifractal indicators and spectral textural features [26]. The resulting texture image enters the classification block for the texture type, where homogeneous image fragments are assigned to the corresponding texture class.

a)   b)   c)

Figure 5. Images of psoriasis on the skin for different types of textures: spectral-statistical a), statistical b) and spectral c).

The developed segmentation modulus of spectral-statistical textures was applied for the

segmentation of psoriatic disease images in DRVIs of automated medical diagnostic systems. In Figure 5, images of psoriasis on the skin are shown, and they can be attributed to different types of textures: spectral-statistical a), statistical b) and spectral c); a selected rectangular fragment of the image that was used to calculate the features is shown.

The results of classifying the psoriatic skin disease texture images in the feature space of the two main components a_1 and a_2 are presented in Figure 6 for different types of textures: spectral-statistical a), statistical b) and spectral c).

a) b) c)
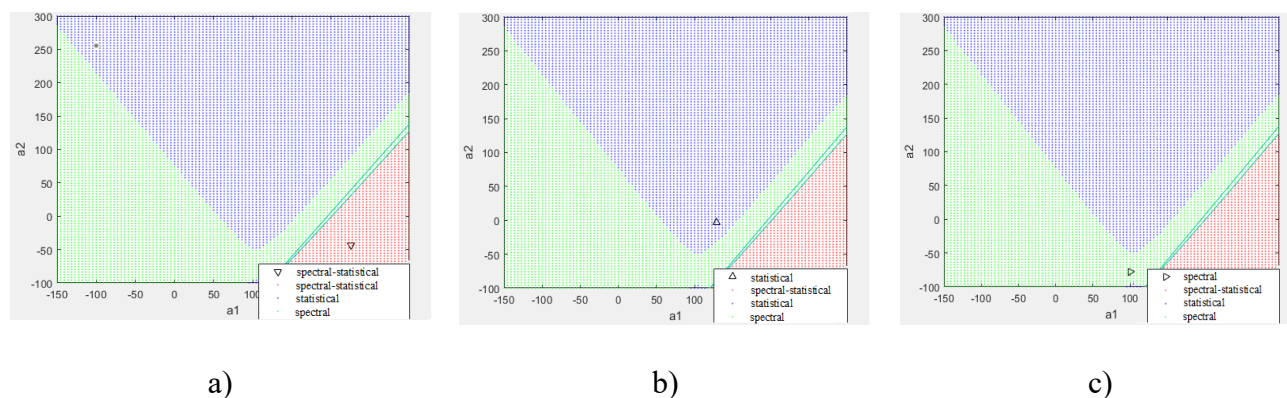
Figure 6. Graphical representation of classification results in the feature space of a_1 and a_2 for texture images of psoriasis: spectral-statistical a), statistical b) and spectral c).

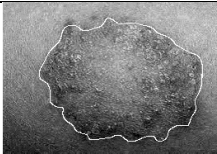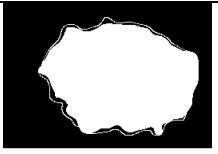**Table 3.** Results of applying segmentation to a psoriasis image.

Input image	Input image with expert markup	Result of segmentation with expert markup	Result of segmentation after contour selection

Table 3 shows example images of psoriatic skin disease with expert markup, and the image obtained by applying the improved vector-difference method of texture segmentation.

The testing results show that the probability of correctly detecting the disease area in the images of psoriatic skin disease was, on average, 0.96, with a probability of a false alarm of 0.05, which is better than the original method [21].

Further, at the stage of identification, the vector of features can be supplemented. The initial data of this stage are the result of tracing the border of the textured area [24] (in this paper-psoriatic spots). It is necessary to determine the features of the shape of textured areas, which are highlighted at the segmentation stage. Currently, the healthcare professional has to manually estimate the perimeter and the area of the psoriatic spot to calculate the indices for further diagnosis. Since there can be many such spots (depending on the degree of disease), an automated system requires both

high efficiency and precise calculations.

When diagnosing psoriasis, the vector of features is subject to the requirements of noise immunity, invariance to scaling, shifting in the field of view and rotation, and sufficient computational efficiency, quality and efficiency.

Such possibilities are provided owing to the identification method, which is based on the geometric moments of features (GMFs) [27]:

$$m_{\alpha\beta} = \int_0^{Lx} \int_0^{Ly} I(x,y) x^\alpha y^\beta \, dxdy, \tag{10}$$

where $I(x,y)$—the image being processed; Lx, Ly—geometric dimensions of the image; α, β—orders of the moment.

The GMF method has a number of advantages. It is characterized by high noise immunity when smoothing the features of moments as integral characteristics. The ensemble of features can be increased to achieve stable recognition.

For recognition, the features, which are based on the GMFs and invariance to scale and rotation, are defined. To do this, the GMFs are calculated in the polar coordinate system:

$$\mu_p = \int_0^{R_{max}} \int_0^{2\pi} \rho^p I(\rho,\phi) d\rho d\phi, \tag{11}$$

where $I(\rho,\phi)$—image brightness function in the polar coordinate system; ρ, ϕ—polar coordinates of the pixels relative to the center of the object weight; p—order of the moment; R_{max}—distance from the center of the figure weight (psoriatic spots) to the most distant point.

In addition, the information on characteristic points [28], was obtained by performing a Lebesgue integration [29]:

$$\mu_p = \iint_A \rho^p Q(\rho,\phi) \psi(x \cap A), \tag{12}$$

where A is the set of real numbers; X is the subset of the coordinates of the characteristic points in the polar coordinate system; ψ—measure of a set of real numbers; Q—set of characteristic points for the contour.

Because the Lebesgue measure in the polar coordinate system is the area of a triangle [28] when the number of characteristic points is large, it is considered that $\sin(\Delta\phi_i) \approx \Delta\phi_i$, and the expression for characteristic points becomes as follows:

$$C_p = \left| \sum_{i=0}^J \rho_{i0}^{(p+2)} \Delta\phi_i \right|. \tag{13}$$

In this paper, the characteristic points are the points of the contour inflection. Since spots with a complex shape can have many such points, an areal method of finding the extrema using the Haar wavelet transform was applied [30]. This method aims to find the extremes of multi-modal objective functions with high noise. Unlike common methods for finding the extrema of such functions (zero, first, second order), the method not only increases the probability of determining the global extremum, but it also improves the performance of such a search. Moreover, the method improves the performance of the procedure for determining the characteristic points of the contour [31], as well as the performance of the identification procedure and diagnosis in dermatological DRVIs. This

method was used for the first time to solve the problem of identification when determining the signs of psoriatic spots. Compared with existing methods based on the first derivative [24], this enhances the noise immunity of the identification procedure and reduces the sensitivity to minor local irregularities in the contour of psoriatic spots (i.e., it reduces the number of characteristic points) due to the smoothing properties of the wavelet transform [32,33]. At the identification stage, this also reduced the variance in the cluster of traits.

Experimental research confirmed that the computational performance of the identification procedure is improved by 1.2 times. The quality of the identification procedure, based on variance, was improved by 1.3 times for the studied set of images.

4. Discussion

This paper presents a significant extension of the method in [21]; this includes the following:

1) A method for the identification of spectral-statistical textures has been proposed; the importance of statistical and spectral texture features is taken into account to increase the probability of the correct detection of the spectral-statistical texture relative to the identification based on the spectral or statistical texture.

2) The model of spectral-statistical textures, as characterized by the value of the background component, random change of spatial frequency and indicators of random field variation, has been improved. In the proposed model, the random change of spatial frequency and field variation are carried out by adding Gaussian noise with a zero mean and variance to the corresponding segment of the image.

3) The improved vector-difference method for spectral-statistical textures was developed for application based on the wavelets at the stage of contour segmentation, which are characterized by low error during the determination of the coordinates of intensity differences; this increases the reliability of homogeneous textured areas.

4) A segmentation modulus of spectral-statistical textures for medical psoriasis images in DRVIs has been developed. The method of identification is implemented in the blocks for identification and classification of the texture type [26].

5) It is proposed to use the geometric moments and features of psoriatic spots at the identification stage after calculating them on the basis of determining the characteristic points of their contour, and by applying Lebesgue integration with a search for the characteristic points using the areal method [30].

The main advantages of the proposed approach as compared to the method in [21] are as follows: (i) the features are invariant to parallel transfers because the zero of the polar coordinate system is combined with the center of gravity of the figure; (ii) features are resistant to scaling because the radius vectors of characteristic points are normalized; (iii) the features are invariant to the angle of rotation of the object; (iv) invariance is provided as a result of summing the results obtained by traversing the contour; high noise immunity of the method is provided by taking into account the smoothing properties of the moments and employing an areal method to search the characteristic points described above; (v) the ensemble of features is easily built up for stable recognition; and (vi) the high computational efficiency of the method due to the small number of processed characteristic points.

We should note that the problem of identifying psoriatic spots is related to the significant

number of features. They are as follows: (i) a large number of variants of the shapes of these spots (perimeter, area) that depend on the damage degree; (ii) the characteristics of methods based on the wavelet transform, which is required to increase the efficiency for the significant number of studies regarding the length of the wavelet function carrier (For example, in the issue of identification, it is influenced by the variability of spot shapes); (iii) it is interesting in this regard to be able to determine the specified parameters of the wavelet function for different coefficients, which is a common technique for determining the severity of the disease for medical professionals.

Taking into account the above, we plan to explore those features in the further research.

5. Conclusions

The analysis of the subject area showed that existing textural segmentation methods do not provide the quality necessary for the practice of segmentation for combined spectral-statistical textures. Therefore, the model of spectral-statistical texture has been improved, the method for the identification of spectral-statistical textures has been developed and the method of vector-difference segmentation for computer-based diagnostic systems in dermatology has been improved. It has been proven that the developed methods provide high-quality texture segmentation and high processing performance compared to the classification methods. The analysis of the classification reliability for homogeneous areas of spectral-statistical textures confirmed the following outcomes. When identifying based on spectral and statistical textures, the probability of correctly detecting the spectral-statistical texture is 1.6 times higher than that based on the spectral texture, and six times higher than that based on the statistical texture at a signal-to-noise ratio of 5 or more. The probability of a false alarm is less than 0.4 when the signal-to-noise ratio is less than 5, and not more than 0.06 when the signal-to-noise ratio is more than 5. The test results confirmed that the probability of the correct detection of the disease area in images of psoriatic skin disease is, on average, 0.96, and the probability of a false alarm is 0.05, which are sufficient for the needs of practice. The proposed procedure for determining the vector of features for the purpose of image recognition in dermatologic diagnostic systems, which is based on processing the characteristic points, reduces the amount of processed data required for sufficient performance and quality.

The conducted research makes it possible to recommend the developed method to be used for investigating psoriatic disease and in adjacent areas of medical diagnostics.

In future research, the authors are going to 1) identify the most informative features based on the characteristic points for different degrees and types of psoriasis, 2) investigate the properties and 3) determine the parameters of the areal method with wavelet transform to solve the problem of segmentation for different degrees of disease.

Acknowledgment

Conflict of interest

The authors declare that the research was conducted in the absence of any commercial or

financial relationships that could be construed as a potential conflict of interest.

References

1. Y. Yemchenko, K. Ischeikin, Features of the clinical course of psoriasis in patients with obesity, *Med. Ecol. Probl.*, **24** (2020), 3–7. https://doi.org/10.31718/mep.2020.24.1-2.01

2. K. G. Paulson, D. Gupta, T. S. Kim, J. R. Veatch, D. R. Byrd, S. Bhatia, et al., Age-specific incidence of melanoma in the United States, *JAMA Dermatol.*, **156** (2020), 57–64. https://doi.org/ 10.1001/jamadermatol.2019.3353.

3. M. J. Schaap, N. J. Cardozo, A. Patel, E. M. G. J. de Jong, B. van Ginneken, M. M. B. Seyger, Image-based automated psoriasis area severity index scoring by convolutional neural networks, *J. Eur. Acad. Dermatol. Venereol.*, **36** (2022), 68–75. https://doi.org/10.1111/jdv.17711

4. S. Gerdes, A. Krber, M. Biermann, C. Karnthaler, M. Reinhardt, Absolute and relative psoriasis area and severity index (PASI) treatment goals and their association with health-related quality of life, *J. Dermatol. Treat.*, **31** (2020), 470–475. https://doi.org/10.1080/09546634.2020.1746734

5. A. U. R. Butt, W. Ahmad, R. Ashraf, M. Asif, S. A Cheema, Computer aided diagnosis (CAD) for segmentation and classification of burnt human skin, in *Proceedings of the 2019 International Conference on Electrical, Communication, and Computer Engineering (ICECCE)*, (2019), 1–5. https://doi.org/10.1109/ICECCE47252.2019.8940758.

6. J. Glaister, A. Wong, Segmentation of skin lesions from digital images using joint statistical texture distinctiveness, *IEEE Trans. Biomed. Eng.*, **61** (2014), 1220–1230. https://doi.org/10.1109/TBME.2013.2297622

7. F. S. Saleh, R. Azmi, Automatic multiple regions segmentation of dermoscopy images, in *Proceedings of the 2015 The International Symposium on Artificial Intelligence and Signal Processing (AISP)*, (2015), 24–29. https://doi.org/10.1109/AISP.2015.7123482

8. Y. Li, Z. Wu, S. Zhao, X. Wu, Y. Kuang, Y. Yan, et al., PSENet: Psoriasis severity evaluation network, in *Proceedings of the The Thirty-Fourth AAAI Conference on Artificial Intelligence (AAAI-20)*, (2020), 800–807. https://doi.org/10.1609/aaai.v34i01.5424

9. E. F. López, Á. M. García, L. S. D. Blanco, J. F. Marinero, J. P. Turiel, Automatic gauze tracking in laparoscopic surgery using image texture analysis, *Comput. Methods Programs Biomed.*, **190** (2020), 1–11. https://doi.org/10.1016/j.cmpb.2020.105378

10. S. Wen, T. M. Kurc, Y. Gao, T. Zhao, J. H. Saltz, W. Zhu, Quality assessment in nucleus segmentation of histopathology image, *J. Pathol. Inf.*, **8** (2017), 1–12. https://doi.org/10.4103/jpi.jpi_43_17

11. M. A. Kassem, K. M. Hosny, R. Damaševičius, M. M. Eltoukhy, Machine learning and deep learning methods for skin lesion classification and diagnosis: A systematic review, *Diagnostics*, **11** (2021), 1390. https://doi.org/10.3390/diagnostics11081390

12. L. Rundo, A. Tangherloni, P. Cazzaniga, M. Mistri, S. Galimberti, R. Woitek, et al., A CUDA-powered method for the feature extraction and unsupervised analysis of medical images, *J. Supercomput.*, **77** (2021), 8514–8531. https://doi.org/10.1007/S11227-020-03565-8

13. V. K. Shrivastava, N. D. Londhe, R. S. Sonawane, J. S. Suri, Computer-aided diagnosis of psoriasis skin images with HOS, texture and color features: A first comparative study of its kind, *Comput. Methods Programs Biomed.*, **126** (2016), 98–109. https://doi.org/10.1016/j.cmpb.2015.11.013

14. M. Hazgui, H. Ghazouani, W. Barhoumi, Genetic programming-based fusion of HOG and LBP features for fully automated texture classification, *Vis. Comput.*, **38** (2022), 457–476. https://doi.org/10.1007/s00371-020-02028-8.

15. S. A. Almola, Find edge map for medical images based on texture characteristics, in *Proceedings of the 2021 International Conference on Communication & Information Technology (ICICT)*, (2021), 7–12. https://doi.org/10.1109/ICICT52195.2021.9568424

16. N. Sharma, A. K. Ray, S. Sharma, K. K. Shukla, S. Pradhan, L. M. Aggarwal, Segmentation and classification of medical images using texture-primitive features: Application of BAM-type artificial neural network, *J. Med. Phys.*, **33** (2008), 119–126. https://doi.org/10.4103/0971-6203.42763

17. T. S. Jarad, A. J. Dawood, Computer-aided diagnosis psoriasis lesion using skin color and texture features, *Int. J. Comput. Digital Syst.*, **7** (2018), 145–154. https://doi.org/10.12785/IJCDS / 070303

18. M. R. Mookiah, J. H. Tan, C. K. Chua, E. Y. Ng, A. Laude, L. Tong, Automated characterization and detection of diabetic retinopathy using texture measures, *J. Mechan. Med. Biol.*, **15** (2015), 1550045. https://doi.org/10.1142/S0219519415500451

19. D. Gornea, D. Popescu, L. Ichim, Remote assessment of flooded areas based on inter-spectral statistical features, in *Proceedings of the 2016 39th International Conference on Telecommunications and Signal Processing (TSP)*, (2016), 707–710. https://doi.org/10.1109/TSP.2016.7760976

20. D. N. Anh, Detection of lesion region in skin images by moment of patch, in *Proceedings of the 2016 IEEE RIVF International Conference on Computing & Communication Technologies, Research, Innovation, and Vision for the Future (RIVF)*, (2016), 217–222. https://doi.org/10.1109/RIVF.2016.7800297

21. V. N. Krylov, N. P. Volkova, Vector-difference texture segmentation method in technical and medical express diagnostic systems, *Herald Adv. Inf. Technol.*, **3** (2020), 174–186. https://doi.org/10.15276/hait.04.2020.2

22. L. A. Soares, K. F. Côco, P. M. Ciarelli, E. O. T. Salles, A class-independent texture-separation method based on a pixel-wise binary classification, *Sensors*, **20** (2020), 5432. https://doi.org/10.3390/s20185432

23. T. Lacombe, H. Favrelière, M. Pillet, Modal features for image texture classification, preprint, arXiv:2005.01928. https://doi.org/10.1016/j.patrec.2020.04.036

24. D. Zahorodnia, Y. Pigovsky, P. Bykovyy, Canny-based method of image contour segmentation, *Int. J. Comput.*, **15** (2016), 200–205. https://doi.org/10.47839/ijc.15.3.853

25. A. Zollanvari, B. Abibullaev, Bias correction for linear discriminant analysis, *Pattern Recognit. Lett.*, **151** (2021), 41–47. https://doi.org/10.1016 / J.PATREC.2021.07.026

26. N. P. Volkova, V. N. Krylov, Hybrid texture identification method, *Herald Adv. Inf. Technol.*, **4** (2021), 123–134. https://doi.org/10.15276/hait.02.2021.2

27. E. Li, Y. Huang, D. Xu, H. Li, Shape DNA: Basic generating functions for geometric moment invariants, preprint, arXiv: 1703.02242. https://arxiv.org/pdf/1703.02242.pdf

28. H. Nasser, P. Ngo, I. Debled-Rennesson, Dominant point detection based on discrete curve structure and applications, *J. Comput. Syst. Sci.*, **95** (2018), 177–192. https://doi.org/10.1016/j.jcss.2017.07.007

29. R. Sjamaar, Lebesgue integration, *All Math You Missed*, (2021), 255–265. https://doi.org/10.1017/9781108992879.016

30. G. Shcherbakova, S. Antoshchuk, A. Sachenko, M. Gerganov, M. Polyakova, V. Krylov, Areal multistart method of optimization for image recognition, in *Proceedings of the IEEE Second International Conference on Data Stream Mining & Processing*, (2018), 605–608. https://doi.org/10.1109/DSMP.2018.8478551

31. G. Shcherbakova, V. Krylov, B. Rusyn, A. Sachenko, P. Bykovyy, D. Zahorodnia, et al., Optimization methods on the wavelet transformation base for technical diagnostic information systems, in *Proceedings of the 11th IEEE International Conference on Intelligent Data Acquisition and Advanced Computing Systems: Technology and Applications (IDAACS'2021)*, (2021), 767–773. https://doi.org/10.1109/IDAACS53288.2021.9660927

32. H. Zhengbing, I. Tereikovskyi, D. Chernyshev, L. Tereikovska, O. Tereikovskyi, W. Dong, Procedure for processing biometric parameters based on wavelet transformations, *Int. J. Mod. Educ. Comput. Sci*, **13** (2021), 11–22. https://doi.org/10.5815/ijmecs.2021.02.02

33. I. Paliy, A. Sachenko, V. Koval, Y. Kurylyak, Approach to face recognition using neural networks, in *Proceedings of the IEEE International Conference on Intelligent Data Acquisition and Advanced Computing Systems: Technology and Applications (IDAACS'2005)*, (2005), 112–115. doi:10.1109/IDAACS.2005.282951